Journal of Hazardous Materials 170 (2009) 1133–1140

Contents lists available at ScienceDirect

Journal of Hazardous Materials

journal homepage: www.elsevier.com/locate/jhazmat

Adsorptive desulfurization by activated alumina

Ankur Srivastav, Vimal Chandra Srivastava *

Department of Chemical Engineering, Indian Institute of Technology Roorkee, Roorkee 247667, India

ARTICLE INFO

Article history:
Received 7 February 2009
Received in revised form 18 May 2009
Accepted 18 May 2009
Available online 22 May 2009

Keywords:
Adsorption
Dibenzothiophene
Alumina
Desulfurization
Kinetic study
Isotherm study
Thermodynamics

ABSTRACT

This study reports usage of commercial grade activated alumina (aluminum oxide) as adsorbent for the removal of sulfur from model oil (dibenthiophene (DBT) dissolved in n-hexane). Bulk density of alumina was found to be 1177.77 kg/m^3. The BET surface area of alumina was found to decrease from 143.6 to 66.4 m^2/g after the loading of DBT at optimum conditions. The carbon-oxygen functional groups present on the surface of alumina were found to be effective in the adsorption of DBT onto alumina. Optimum adsorbent dose was found to be 20 g/l. The adsorption of DBT on alumina was found to be gradual process, and quasi-equilibrium reached in 24 h. Langmuir isotherm best represented the equilibrium adsorption data. The heat of adsorption and change in entropy for DBT adsorption onto alumina was found to be 19.5 kJ/mol and 139.2 kJ/mol K, respectively.

1. Introduction

Presence of sulfur compounds in crude oil is making a great hole in refiners' pocket the world over. The issues of deep desulfurization are becoming more serious because of the increase in sulfur content of the crude oil and lowering of the regulated sulfur limits in diesel and gasoline [1]. According to the recently announced Euro V norms, the fuel sulfur content will have to be reduced to as low as 10 ppm in near future. With the latest regulations in India to reduce the gasoline sulfur content from current maximum of 150 to 50 ppm by 2010, and to cut the diesel sulfur content from current 350 to 50 ppm by 2010, refineries in India are facing major challenges to meet the fuel sulfur specification along with the required reduction of aromatics contents [2].

Various desulfurization techniques like hydrodesulfurization (HDS), oxidative desulfurization (ODS), bio-desulfurization (BDS) and adsorptive desulfurization are being investigated world over to produce ultra clean fuels. HDS is the most commonly used method of sulfur reduction of fossil fuels in refineries. Typically, it involves catalytic treatment with hydrogen to convert the various sulfur compounds to hydrogen sulfide [3]. However, it requires the application of severe operating conditions and the use of especially activated catalysts for the production of fuels with very low levels of sulfur compounds [4,5]. HDS is limited in treating benzothiophenes (BTs) and dibenzothiophenes (DBTs), especially DBTs having alkyl substituent on 4 and/or 6 positions. Moreover, the HDS process has reached a stage where increasing temperature and pressure are just not enough to remove last traces of sulfur without affecting the octane number. In the oxidation process, the sulfur containing compounds is oxidized to sulfone by chemical reaction using various types of oxidants namely H_2O_2, H_2SO_4, etc. The sulfone compound is then easily extracted from the fuel because of its higher polarity [6–11]. Reaction selectivity, safety and cost are important concerns for the selection of oxidants, catalysts and operating conditions in ODS processing. The catalytic systems reported in literature are mostly toxic and expensive. Bio-desulfurization has drawn wide attention over the past decade. Considerable research has been done to extend the understanding of the enzymology and molecular genetics of the BDS system and to apply that into the design of the BDS bioreactor and bioprocesses [12–15].

In the adsorptive desulfurization technique, the active adsorbent is placed on a porous, non-reactive substrate that allows high surface area for the adsorption of sulfur compounds. Adsorption occurs when the sulfur molecules attach to the adsorbent and remain there separate from the fuel. Various investigators have utilized this technique for the removal of sulfur from various types of fuels and model oils by various types of adsorbents [16–22]. Desulfurization by adsorption faces the challenge of developing easily remunerable adsorbent with a high adsorption capacity. Adsorbents developed must have high selectivity for the adsorption of refractory aromatic sulfur compounds that do not get removed during the HDS process.

Alumina has good adsorptive properties and has been used for the removal of organic compound from aqueous solutions [23]; and surfactants like sodium dodecyl and octylphenol from single and in

* Corresponding author. Tel.: +91 1332 285889; fax: +91 1332 276535/273560.
E-mail address: vimalcsr@yahoo.co.in (V.C. Srivastava).

0304-3894/$ – see front matter © 2009 Elsevier B.V. All rights reserved.
doi:10.1016/j.jhazmat.2009.05.088

multi-surfactant aqueous solutions [24]. Various researchers have utilized it for the adsorptive removal of phosphate [25]; Co(II), Ni(II), Cu(II), and Cr(II) [26]; Zn(II) [27]; and dibenzothiophene sulfone, etc. [28].

In a recent study, Etemadi and Yen [28] utilized various characterization techniques to explain the difference in the adsorption capacity of amorphous acidic alumina and crystalline boehmite for the adsorption of DBT sulfone in ultrasound-assisted oxidative desulfurization process. Kim et al. [29] studied the adsorptive desulfurization using a model diesel fuel over three typical adsorbents (activated carbon, activated alumina and nickel-based adsorbent) in a fixed-bed adsorption system. However, no attempt was made to study the engineering aspects like kinetics, isotherm and thermodynamics of the adsorption process. Also, very few adsorptive desulfurization studies have focused on these engineering aspects which are important in designing adsorption system.

In the present study, commercial grade alumina has been explored for the removal of sulfur from model oil (DBT dissolved in n-hexane). Alumina has been characterized for its physico-chemical characteristics such as surface area and surface functional groups. X-ray and energy dispersive diffractograms, scanning electron micrograph (SEM), and Fourier transform infra-red (FTIR) spectra have been used to understand the mechanism of DBT adsorption onto alumina. The present study also reports the effect of such factors as the pH, adsorbent dose (m), initial DBT concentration (C_0), and contact time (t) on the adsorption efficiency of DBT by alumina. The kinetics of adsorption has been studied, and various kinetic models, such as pseudo-first-order, pseudo-second-order, and diffusion models have been tested with experimental data for their validity. The equilibrium sorption behaviour of the adsorbents has been studied using the adsorption isotherm technique. Experimental data have been fitted to various isotherm equations to determine the best isotherm to correlate the experimental data. Thermodynamics of adsorption process has been studied and the changes in Gibbs free energy, enthalpy and the entropy have been determined.

2. Materials and methods

2.1. Adsorbent and its characterization

Activated alumina was supplied by S.D. Fine Chemicals, Mumbai, India. It was used as procured. The physico-chemical characterization of alumina was performed using standard procedures. Proximate analysis of the alumina was carried out as per IS 1350: 1984 [30]. Bulk density was determined using MAC bulk density meter.

To understand the morphology of the alumina, a scanning electron microscope (SEM) QUANTA, Model 200 FEG, USA was used. Sample was first gold coated using Sputter Coater, Edwards S150, which provides conductivity to the samples, and then the SEMs and energy dispersive X-ray (EDX) spectra were taken.

The structure of alumina was studied with the help of an X-ray diffractometer (Bruker AXS, Diffractometer D8, Germany). XRD analysis was done using Cu-Kα as a source and Ni as a filter media, and K radiation maintained at 1.542 Å. Goniometer speed was kept at $2^\circ\,\mathrm{min}^{-1}$. The range of scanning angle (2θ) was kept at 10–90°. The intensity peaks indicate the values of 2θ, where Bragg's law is applicable. The identification of compounds was done using the ICDD library.

Textural characteristic of the alumina was determined by nitrogen adsorption at 77.15 K using an automatic Micromeritics Chemisorb 2720, Pulse Chemisorption System. The Brunauer–Emmett–Teller (BET) surface area [31] and monolayer pore volume of the alumina before and after adsorption of DBT was determined using the software available with the instrument.

2.2. Adsorbate

All the chemicals used in the study were of analytical reagent (AR) grade. DBT was procured from Merck, Germany. N-hexane was obtained from S.D. fine Chemicals, Mumbai, India. Stock solution of sulfur having 1 g/l concentration was made by dissolving 5.77 g of DBT in 1 l n-hexane. The range of concentration of sulfur solutions prepared from stock solution by diluting with n-hexane varied between 100 and 1000 mg/l.

2.3. Batch adsorption studies

For each experimental run, 50 ml solution of known sulfur concentration was taken in 100 ml conical flask containing pre-weighed amount of alumina. These flasks were agitated at a constant shaking rate of 120 rpm in a temperature controlled orbital shaker (Remi Instruments, Mumbai) maintained at 30 °C except for the experiments carried out to test the effect of temperature. The flasks were withdrawn at the end of predetermined time (t) and the supernatant liquid was analyzed for residual sulfur concentration.

Adsorption kinetics was followed for 6 days for sulfur solutions having C_0 values of 100, 200, 500 and 1000 mg/l.

2.4. Analysis of DBT

The concentration of DBT in the sample was determined by using Gas Chromatograph (GC) equipped with flame ionization detector (FID). Before the analysis, the sample was diluted to the concentration in the range of 0–2.875 g/l for DBT with n-Hexane. DBT concentrations were determined in reference to the appropriate standard DBT solutions.

The percentage removal of sulfur and equilibrium adsorption uptake in the solid phase (q_e (mg/g)) were calculated using the following relationships:

$$\text{Percentage sulfur removal} = \frac{100\ (C_0 - C_e)}{C_0} \tag{1}$$

Amount of adsorbed sulfur per gram of solid,

$$q_e = \frac{(C_0 - C_e)}{m} \tag{2}$$

where, C_0 is the initial sulfur concentration (mg/l), C_e is the equilibrium sulfur concentration (mg/l) and m is the adsorbent dose in grams per litre of solution.

2.5. Adsorption kinetic theory

2.5.1. Pseudo-first-order- and pseudo-second-order-model

The adsorption of DBT molecules from oil phase to the solid phase can be considered as a reversible process with equilibrium being established between the solution and the solid phase. Assuming non-dissociating molecular adsorption of DBT molecules on alumina particles with no DBT molecules initially present on the adsorbent, the uptake of the DBT molecules by the alumina at any instant (t) is given as [32]

$$q_t = q_e[1 - \exp(-k_f t)] \tag{3}$$

where, q_e = amount of the adsorbate adsorbed on the adsorbent under equilibrium condition and k_f is the pseudo-first-order rate constant.

The pseudo-second-order model is represented as: [33,34]

$$q_t = \frac{tk_S q_e^2}{1 + tk_S q_e} \tag{4}$$

The initial adsorption rate, h (mg/g min), at $t \to 0$ is defined as

$$h = k_S q_e^2 \quad (5)$$

2.5.2. Diffusion study

The possibility of intra-particle diffusion was explored by using the intra-particle diffusion model [35].

$$q_t = k_{id} t^{1/2} + I \quad (6)$$

where, k_{id} is the intra-particle diffusion rate constant, and values of I give an idea about the thickness of the boundary layer.

In order to check whether surface diffusion controlled the adsorption process, the kinetic data were further analyzed using Boyd kinetic expression which is given by [36,37]:

$$F = 1 - \frac{6}{\pi^2} \exp(-B_t) \text{ or } B_t = -0.4977 - \ln(1 - F) \quad (7)$$

where, $F(t) = q_t/q_e$ is the fractional attainment of equilibrium at time t, and B_t is a mathematical function of F.

2.6. Adsorption equilibrium study

Equilibrium adsorption equations are required in the design of an adsorption system and their subsequent optimization. Therefore it is important to establish the most appropriate correlation for the equilibrium isotherm curves. Srivastava et al. [38] have discussed the theory associated with the most commonly used isotherm models. We tried to use the four isotherm equations namely Freundlich [39], Langmuir [40], Redlich-Peterson (R-P) [41] and Temkin [42] and R-P to fit the experimental data for DBT adsorption onto alumina at various temperatures. For each system and each isotherm equation, all the experimental data were used. The Marquardt's percent standard deviation (MPSD) error function [43] was employed in this study to find out the most suitable kinetic and isotherm model to represent the experimental data. This error function is given as

$$\text{MPSD} = 100 \sqrt{\frac{1}{n_m - n_p} \sum_{i=1}^{n} \left(\frac{q_{e,i,\text{exp}} - q_{e,i,cal}}{q_{e,i,\text{exp}}} \right)^2} \quad (8)$$

In this equation, the subscript 'exp' and 'calc' represent the experimental and calculated values, n_m is the number of measurements, and n_p is the number of parameters in the model.

3. Results and discussion

3.1. Characterization of alumina

Average particle size of alumina was 0.074 mm. Proximate analysis showed the presence of 1.99% moisture, 0.23% volatile matter and 97.78% ash in alumina. Chemical analysis of the ash of alumina showed the presence of Al_2O_3 (99%), SiO_2 (0.41%), and rest others. Bulk density of alumina was found to be 1177.77 kg/m^3.

The SEM of the alumina is shown in Fig. 1. It shows that alumina is an aggregate of small crystalline structure of average dimension of ~10 μm. This figure reveals surface texture and porosity of the blank alumina.

XRD of blank alumina was also carried out (Fig. 2). The d-spacing values provided by the XRD spectra of alumina reflected the presence of aluminum oxide and boehmite as major components. Peaks of DBT were observed in DBT loaded alumina.

The BET surface area of blank, and DBT loaded alumina were found to be 143.6 and 66.4 m^2/g, respectively. Corresponding monolayer volumes were found to be 33 and 15.24 cm^3/g, respectively. The decrease in BET surface area and monolayer volume of alumina is due to the loading of DBT.

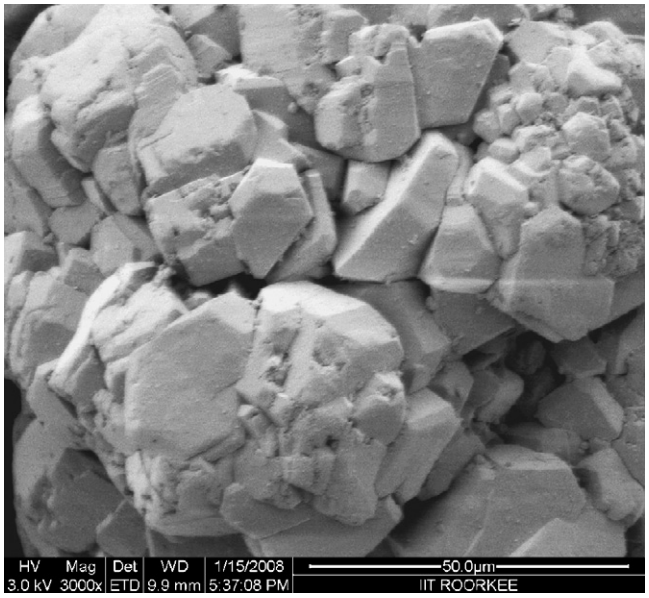

Fig. 1. Scanning electron micrograph of blank alumina.

The energy dispersive spectrum (EDX) of alumina before and after adsorption of DBT showed the presence of 46.2% and 45.4% oxygen; 53.8% and 52.9% aluminum, respectively, in blank and DBT loaded alumina. In addition, DBT loaded alumina was found to contain 1.2% carbon and 0.5% sulfur. Sulfur content is due to the loading of DBT on alumina.

3.2. Effect of alumina dosage (m)

The effect of m on the uptake of DBT onto alumina was studied at $T = 303$ K and $C_0 = 500$ mg/l and the results are shown in Fig. 3. The removal of DBT was found to be increasing with an increase in the m from 1 to 20 g/l. The removal remained unchanged for $m > 20$ g/l for alumina. The increase in the adsorption with the alumina dosage can be attributed to the availability of greater surface area and more adsorption sites. At $m < 15$ g/l, the alumina surface becomes saturated with DBT and the residual DBT concentration in the solution is large. With an increase in m, the DBT removal increases due to increased DBT uptake by the increased amount of alumina. For $m > 15$ g/l, the incremental DBT removal became low. At about $m = 20$ g/l, the removal efficiency became almost constant at for DBT removal by alumina.

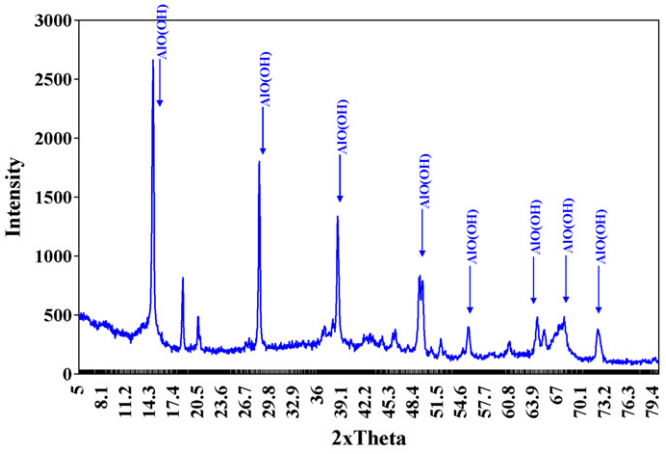

Fig. 2. XRD pattern of blank alumina.

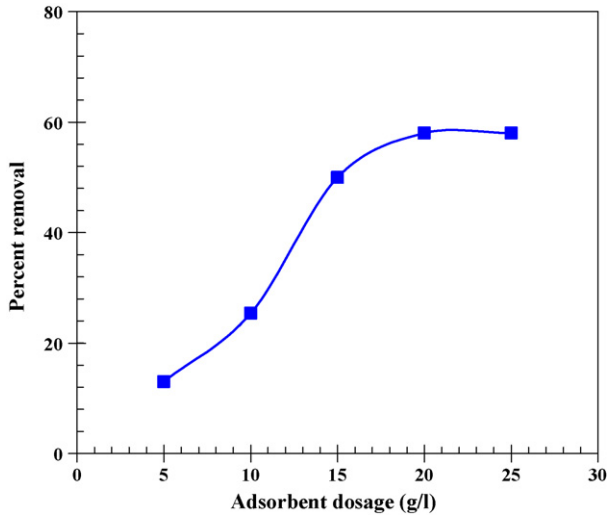

Fig. 3. Effect of adsorbent dose on the removal of DBT by alumina. T = 303 K, C_0 = 500 mg/l.

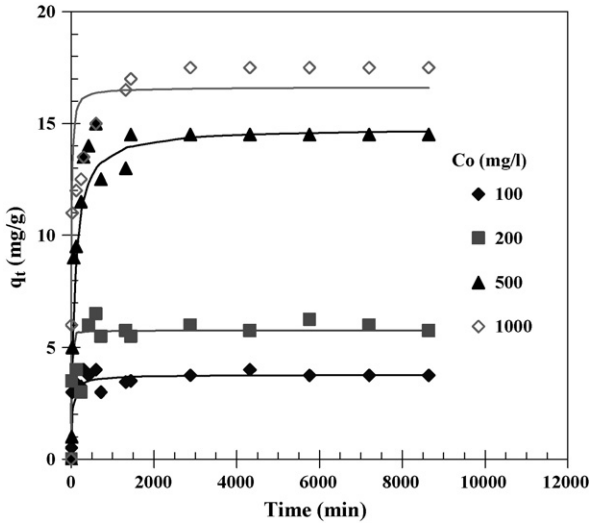

Fig. 5. Effect of contact time on the removal of sulfur by alumina. Experimental data points given by the symbols and the lines predicted by the pseudo-second-order model. T = 303 K, m = 20 g/l.

3.3. Effect of DBT concentration (C_0)

The effect of C_0 on the extent of adsorption of DBT onto alumina at m = 20 g/l is shown in Fig. 4. It is evident that the DBT removal decreases with an increase in C_0, although the actual amount of DBT adsorbed per unit mass of alumina increased with an increase in C_0. The amount adsorbed increased with an increase in the adsorbate concentration due to the decrease in the resistance for the uptake of DBT from the solution.

3.4. Effect of contact time

The rate and quantity of adsorbate adsorbed by the adsorbent is limited by the size of adsorbate molecules, concentration of adsorbate and its affinity towards the adsorbent, diffusion coefficient of the adsorbate in the bulk and solid phase, the pore size distribution of the adsorbent, and degree of mixing. DBT solutions with different C_0 (=100, 200, 500 and 1000 mg/l) were kept in contact with alumina for 6 days. Fig. 5 presents a representative plot of the time-course of DBT onto alumina. The residual concentrations at 24 h contact time were found to be varied by a maximum of ~1% than those obtained after 6 days contact time. Therefore, after 24 h contact time, a steady state approximation was assumed and a quasi-equilibrium situation was accepted. Accordingly all the batch experiments were conducted with a contact time of 24 h under vigorous shaking conditions. The rate of DBT removal is found to be very rapid during the initial 30 min, and thereafter, the rate of DBT removal decreases. It is found that the adsorptive removal of the DBT ceases after 24 h of contacting with alumina. A large number of vacant surface sites are available for adsorption during the initial stage, and after a lapse of time, the remaining vacant surface sites are difficult to be occupied due to repulsive forces between the solute molecules on the solid and bulk phases. Besides, the DBT is adsorbed into the macro- and meso-pores that get almost saturated with DBT during the initial stage of adsorption. Thereafter, the DBT molecules have to traverse farther and deeper into the micro-pores encountering much larger resistance. This results in the slowing down of the adsorption during the later period of adsorption.

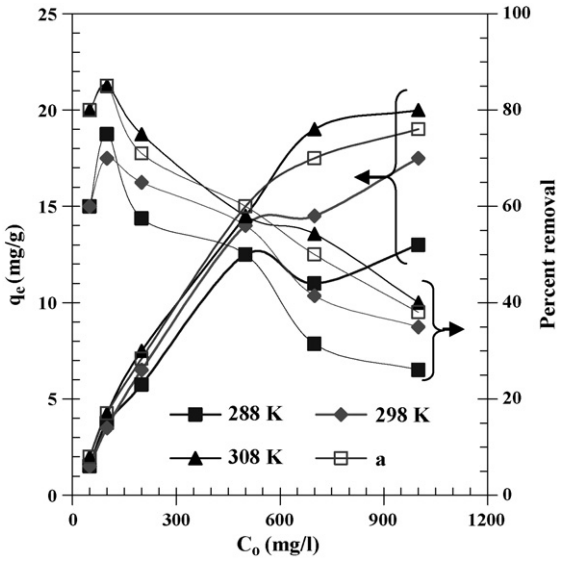

Fig. 4. Effect of initial sulfur concentration on the removal of sulfur by alumina.

3.5. Adsorption kinetic study

The prediction of the batch adsorption kinetics is necessary for the design of industrial adsorption columns. In the present study, the frequently used kinetic models, namely pseudo-first-order and pseudo-second-order models have been tested to investigate the adsorption of DBT onto alumina. The best-fit values of k_f, h and k_S along with coefficient of determination and MPSD for the pseudo-first-order and pseudo-second-order models for DBT adsorption onto alumina with C_0 = 100, 200, 500 and 1000 mg/l at 303 K is given in Table 1. The $q_{e,exp}$ and the $q_{e,cal}$ values for the pseudo-first-order model and pseudo-second-order models are also shown in Table 1. The $q_{e,exp}$ and the $q_{e,cal}$ values from the pseudo-second-order kinetic model are very close to each other. The calculated coefficient of determination are also closer to unity for pseudo-second-order kinetics than that for the pseudo-first-order kinetic model. Therefore, the adsorption can be approximated more appropriately by the pseudo-second-order kinetic model than the pseudo-first-order kinetic model for the adsorption of DBT onto alumina. It may, however, be pointed out that the difference in prediction by the two models is small, and any of the two could be used for kinetic modeling.

Table 1
Kinetic parameters for the removal of sulfur by alumina. C_0 = 100–1000 mg/l, m = 20 g/l.

Pseudo-first-order model					
C_0 (mg/l)	$q_{e,exp}$ (mg/g)	$q_{e,cal}$ (mg/g)	k_f (min^{-1})	R^2	MPSD
100	3.75	3.75	0.0286	0.9536	43.44
200	5.75	5.75	0.0099	0.8370	78.89
500	14.50	14.50	0.0080	0.9732	70.95
1000	17.50	16.50	0.0904	0.9092	65.49
Pseudo-second-order model					
C_0 (mg/l)	$q_{e,calc}$ (mg/g)	k_S (g/mg min)	h (mg/g min)	R^2	MPSD
100	3.76	0.0081	0.12	0.9256	54.51
200	5.75	0.0540	1.78	0.8653	64.71
500	14.78	0.0008	0.17	0.9729	94.73
1000	16.61	0.0068	1.88	0.9463	49.70
W-M Intra-particle diffusion model					
C_0 (mg/l)	$k_{id,1}$ (mg/g min$^{1/2}$)		I_1 (mg/g)	R^2	
100	0.158		1.323	0.567	
200	0.170		1.654	0.575	
500	0.145		9.312	0.515	
1000	0.185		10.02	0.976	
C_0 (mg/l)	$k_{id,2}$ (mg/g min$^{1/2}$)		I_2 (mg/g)	R^2	
100	0.001		3.613	0.026	
200	0.005		5.489	0.191	
500	0.004		14.21	0.538	
1000	0.013		16.41	0.596	

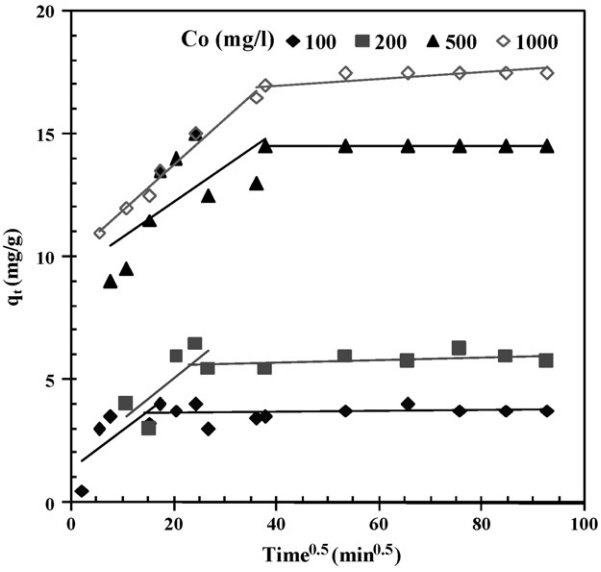

Fig. 6. Weber and Morris intra-particle diffusion plot for the removal of sulfur by alumina. T = 303 K, m = 20 g/l.

3.6. Diffusion study

The transport of adsorbate from the solution phase into the pores of the adsorbent particles may be controlled either by one or more steps, e.g. film or external diffusion, pore diffusion, surface diffusion and adsorption on the pore surface, or a combination of more than one step. It is necessary to calculate the slowest step involved in the adsorption process. For adsorption process, the external mass transfer controls the sorption process for the systems that have poor mixing, dilute concentration of adsorbate, small particle sizes of adsorbent and higher affinity of adsorbate for adsorbent. Whereas, the intra-particle diffusion controls the adsorption process for a system with good mixing, large particle sizes of adsorbent, high concentration of adsorbate and low affinity of adsorbate for adsorbent [44].

In general, external mass transfer is characterized by the initial solute uptake [45] and can be calculated from the slope of plot between C/C_0 versus time. The slope of these plots can be calculated either by assuming polynomial relation between C/C_0 and time or it can be calculated based on the assumption that the relationship was linear for the first initial rapid phase (in the present study first 30 min). In the present study, the second technique was used by assuming the external mass transfer occurs in the first 30 min. The initial adsorption rates (K_s) (min^{-1}) were quantified as $(C_{30min}/C_0)/30$. The calculated K_s values were found to be 0.02, 0.0095, 0.0067 and 0.0063 min^{-1} for an initial dye concentration of 100, 200, 500 and 1000 mg/l, respectively.

If the Weber–Morris plot of q_t versus $t^{0.5}$ satisfies the linear relationship with the experimental data, then the adsorption process is found be controlled by intra-particle diffusion only. However, if the data exhibit multi-linear plots, then two or more steps influence the overall adsorption process. Fig. 6 shows a representative q_t versus $t^{0.5}$ plot for DBT ion adsorption onto alumina for C_0 = 100, 200, 500 and 1000 mg/l at 303 K and pH_0 6.0. In this figure, the plots are not linear over the whole time range, implying that the more than one process is controlling the adsorption process. The first portion (line not drawn for the clarity of picture) gives the diffusion of adsorbate through the solution to the external surface of adsorbent or boundary layer diffusion. Further two linear portions depict intra-particle diffusion. The second linear portion is attributed to the gradual equilibrium stage with intra-particle diffusion dominating. The third portion is the final equilibrium stage for which the intra-particle diffusion starts to slow down due to the extremely low adsorbate concentration left in the solution [46,47]. Extrapolation of the linear portions of the plots back to the y-axis gives the intercepts that provide the measure of the boundary layer thickness. The deviation of straight lines from the origin indicates that the pore diffusion is not the sole rate-controlling step. Therefore, the adsorption proceeds via a complex mechanism [48] consisting of both surface adsorption and intra-particle transport within the pores of alumina. The slope of the linear portions are defined as a rate parameters ($k_{id,1}$ and $k_{id,2}$) and are characteristics of the rate of adsorption in the region where intra-particle diffusion is rate controlling. It can be inferred from the Fig. 6 that the diffusion of DBT from the bulk phase to the external surface of alumina, which begins at the start of the adsorption process, is the fastest. It seems that the intra-particle diffusion of DBT into micro-pores (third portion) is the rate-controlling step in the adsorption process. The third portion of the plots is nearly parallel ($k_{id,2} \approx 0.001$–0.013 mg/g min$^{0.5}$), suggesting that the rate of adsorption DBT into the micro-pores of alumina is comparable at all C_0. Slopes of second and third portions ($k_{id,1}$ and $k_{id,2}$) are higher for higher C_0, which corresponds to an enhanced diffusion of DBT through meso- and micro-pores. This is due to the greater driving force at higher C_0.

The multi-phasic nature of intra-particle diffusion plot confirms the presence of both film and pore diffusion. In order to predict the actual slow step involved, the kinetic data were further analyzed using Boyd kinetic expression. Eq. (7) was used to calculate B_t values at different time t. The linearity of the plot of B_t versus time was used to distinguish whether external and intra-particle transport controls the adsorption rate. It was observed that the relation between B_t and t (not shown here) was non-linear (R^2 = 0.1483–0.8215) at all concentrations, confirming that surface diffusion is the not the sole rate-limiting step. Thus, both film and pore diffusion seem to be the rate-limiting step in the adsorption process and the adsorption proceeds via a complex mechanism.

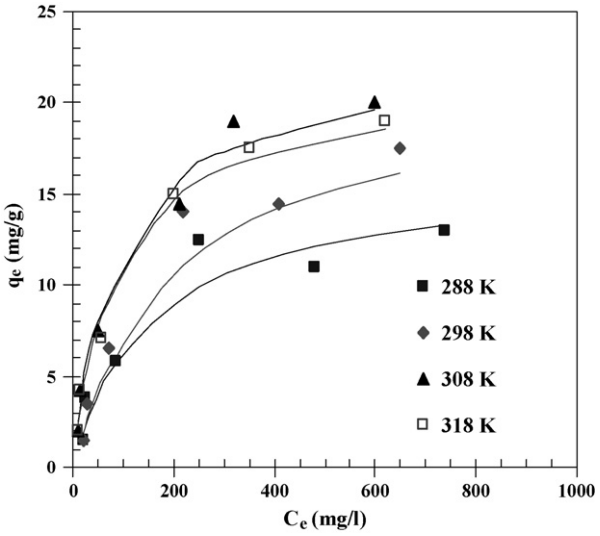

Fig. 7. Equilibrium adsorption isotherms at different temperature. Experimental data points given by the symbols and the lines predicted by the Langmuir model. C_0 = 100–1000 mg/l, m = 20 g/l.

3.7. Adsorption equilibrium study

Fig. 7 shows the adsorption isotherms, q_e versus C_e, at different temperatures ranging from 298 to 328 K. It was found that the adsorption of DBT increases with an increase in temperature. At low adsorbate concentrations, q_e rises sharply. At higher values of C_e, the increase in q_e is gradual. If the adsorption process is controlled by the diffusion process (intra-particle transport-pore diffusion), the adsorption capacity increases with an increase in temperature due to endothermicity of the diffusion process [32]. An increase in temperature results in an increased mobility of the adsorbate and a decrease in the retarding forces acting on the diffusing molecules. This results in the enhancement in the adsorptive capacity of the alumina for the DBT molecules.

The isotherm constants for the four isotherms studied, and the coefficient of determination, R^2 with the experimental data are listed in Table 2. The R^2 values for Langmuir isotherm are closer to unity in comparison to the values obtained for other isotherms, and also the MPSD error values are least for the fit of Langmuir isotherm. Therefore, Langmuir is the best-fit isotherm equation for the adsorption of DBT at all temperatures. Fig. 7 presents how well the Langmuir isotherm fits the data for DBT–alumina system at all temperatures.

3.8. Statistical adsorption thermodynamics

The adsorption of an adsorbate A from a liquid phase onto a solid phase (referred as S) can be depicted by following equation:

$$A + S \rightleftharpoons A \cdot S$$

Let S be the system in the ensemble and the solvent that contains the adsorbate A as donor particles be the medium. Considering the adsorption process as the process of distribution of donor particles to the system, and applying the model of a variable number of particles in statistical physics [49] the probability of distribution of a variable number of particles, for adsorption systems of such a type, is given by [50]

$$\omega(i, \in) = B \exp\left(\frac{i\mu - \in_i}{\gamma}\right) \quad (9)$$

where, B is the normalizing coefficient, μ the chemical potential (which is dependent on the temperature and concentration of the donor particles), i the number of donor particles distributed in the system, γ the distribution module, $\in_i$ the energy of the system that contains i donor particles (which is assumed to be approximately equal for the systems that contain the same number i of donor particles), and $\in_i = 0$ at $i = 0$. The derivation, as given below, is taken from Wang and Jiang [49].

Table 2
Isotherm parameters for the removal of sulfur by alumina. C_0 = 50–1000 mg/l, m = 20 g/l.

Freundlich		$q_e = K_F C_e^{1/n}$		
T (K)	K_F ((mg/g)/(l/mg)$^{1/n}$)	$1/n$	R^2	MPSD
288	0.3593	0.5651	0.9069	34.0130
298	0.2520	0.6799	0.9472	30.3978
308	0.7010	0.5507	0.9690	23.6928
318	0.7184	0.5354	0.9665	23.1256

Langmuir		$q_e = \frac{q_m K_L C_e}{1+K_L C_e}$		
T (K)	q_m (mg/g)	K_L (l/mg)	R^2	MPSD
288	16.07	0.0065	0.9611	25.89
298	21.02	0.0051	0.9880	22.39
308	22.58	0.0109	0.9915	15.27
318	21.25	0.0112	0.9936	17.14

Temkin		$q_e = B_T \ln K_T + B_T \ln C_e$		
T (K)	K_T (l/mg)	B_T (kJ/mol)	R^2	MPSD
288	12.07	0.37	0.9597	74.96
298	15.13	0.35	0.9918	80.07
308	17.15	0.53	0.9891	73.37
318	16.86	0.53	0.9887	72.01

Redlich-Peterson		$q_e = \frac{K_R C_e}{1+a_R C_e^{\beta}}$			
T (K)	K_R (l/g)	a_R (l/mg)$^{1/\beta}$	β	R^2	MPSD
288	0.104	0.0065	0.999	0.9610	29.91
298	0.101	0.0040	0.999	0.9836	23.66
308	0.262	0.0192	0.917	0.9928	17.30
318	0.274	0.0320	0.851	0.9931	18.67

Applying the normalization condition $\left(\sum_{i=0}^{n} \omega(i, \in) = 1\right)$ to the distribution given by Eq. (9), the average number of donor particles accepted by each system is given by [49]

$$\tilde{n} = \sum_{i=1}^{n} i\omega(i, \in) = \sum_{i=1}^{n} iB \exp\left(\frac{i\mu - \in_i}{\gamma}\right) \quad (10)$$

Using Eqs. (11) and (12) to eliminate B, one obtains

$$\tilde{n} = \frac{\sum_{i=1}^{n} i \exp(i\mu - \in_i/\gamma)}{1 + \sum_{i=1}^{n} i \exp(i\mu - \in_i/\gamma)} \quad (11)$$

Considering the fraction of the solute adsorbed from solution (2) as equal to the statistical average value in (0, 1) distribution, Eq. (11) gets reduced to

$$\tilde{n} = \eta = \frac{1}{1 + \exp(\in - \mu/\gamma)} \quad (12)$$

Here, $0 \le \tilde{n} \le 1$. Considering the fact that η is related to the concentration of adsorbate for a fixed dosage of adsorbent and $\in$ is associated with the change of free energy of adsorption G^o, the following equation can be derived from Eq. (14):

$$\ln\left(\frac{1-\eta}{\eta}\right) = \frac{\Delta G^o}{\gamma} + \frac{RT \ln C}{\gamma} \quad (13)$$

The value of γ was estimated from the slope of the plot of $\ln[(1-\eta)/\eta]$ versus $\ln C$ (not shown here) at all the temperatures enabling the determination of ΔG^o values from the ordinate axis intercept of the straight line.

Table 3
Thermodynamics parameters for the removal of sulfur by alumina. C_0 = 50–1000 mg/l, m = 20 g/l.

Temp. (K)	ΔG_0 (kJ/mol)	ΔH_0 (kJ/mol)	ΔS_0 (kJ/mol K)
288	−20.34	19.54	139.18
298	−21.95		
308	−23.86		
318	−24.34		

According to classical thermodynamics, the Gibbs free energy change ΔG^o is also related to the entropy change (ΔS^o) and the heat of adsorption (ΔH^o) at a constant temperature (T) by the following equation:

$$\Delta G^o = \Delta H^o - T\ \Delta S^o \quad (14)$$

Considering the fact that the values of enthalpy and entropy changes of the adsorption process have no distinct changes in the temperature range studied, a plot of ΔG^o versus T enables to determine the values of ΔS^o and ΔH^o.

The values of ΔG^o, ΔH^o and ΔS^o for DBT–alumina system is shown in Table 3. ΔG^o values were negative indicating that the sorption process led to a decrease in Gibbs free energy and that the adsorption process is feasible and spontaneous. The adsorption of DBT onto alumina is endothermic in nature, giving a positive value of ΔH^o. The adsorption process in the DBT–alumina–hexane system is a combination of two processes: (a) the desorption of the solvent (hexane) molecules previously adsorbed, and (b) the adsorption of the adsorbate species. The DBT molecules have to displace more than one hexane molecule for their adsorption, and this results in the endothermicity of the adsorption process. Therefore, ΔH^o is positive. The positive value of ΔS^o suggests increased randomness at the solid/solution interface with some structural changes in the adsorbate and the adsorbent and an affinity of the adsorbent towards DBT.

4. Conclusion

The present study shows that the alumina could be used as adsorbent for the desulfurization of liquid fuels. SEM, EDX, XRD and FTIR studies were performed to understand the mechanism of DBT adsorption onto alumina. Presence of DBT on the surface of alumina was confirmed by comparing EDX of DBT loaded alumina. Equilibrium between the DBT in the solution and on the alumina surface was practically achieved in 24 h. The adsorption processes was well described by a multi-stage diffusion model. The DBT uptake was found to be controlled by external mass transfer at earlier stages and by intra-particle diffusion at later stages. Langmuir isotherm best represented the equilibrium adsorption data at all temperatures. The adsorption of DBT onto alumina was found to be endothermic in nature with the heat of adsorption being 19.5 kJ/mol.

Acknowledgements

Authors are thankful to the Ministry of Human Resource and Development, Government of India, for providing financial support to undertake the work. One of the author, VCS, is thankful to IIT Roorkee for providing financial grant for carrying out this research work.

References

[1] C. Song, An overview of new approaches to deep desulfurization for ultra-clean gasoline, diesel fuel and jet fuel, Catal. Today 86 (2003) 211–263.
[2] Auto Fuel Policy, Ministry of petroleum and Natural gas, Government of India, 2003 (http://petroleum.nic.in/autoeng.pdf).
[3] H. Nikkolaj, M. Brosrson, T. Henrik, Activities of unsupported second transition series metal sulfides for hydrodesulfurization of sterically hindered 4,6 DMDBT and of unsubstituted DBT, Catal. Lett. 65 (2000) 174–196.
[4] J.G. Michael, C.C. Bruce, Reactivities reaction networks, and kinetic in high pressure catalytic hydroprocessing, Ind. Eng. Chem. Res. 30 (1991) 2021–2058.
[5] K. Heeyeon, J. Jung, S. Lee, M. Heup, Hydrodesulfurization of dibenzothiophene compounds using fluorinated $NiMo/Al_2O_3$ catalysts, Appl. Catal. B-Environ. 44 (2003) 287–299.
[6] G.E. Dolbear, E.R. Skov, Selective oxidation as a route to petroleum desulfurization, Am. Chem. Soc. Div. Fuel Chem. 45 (2000) 375–378.
[7] R.T. Yang, A. Takahashi, F.H. Yang, A. Maldonado, Selective sorbents for desulfurization of liquid fuels, U.S. and Foreign Patent applications, 2002.
[8] R.F. Zaykina, Y.A. Zaykin, T.B. Mamaonava, N.K. Nadirov, Radiation methods for demercaptanization and desulfurization of oil products, Radiat. Phys. Chem. 63 (2002) 621–624.
[9] G. Yu, S. Lu, H. Chen, Z. Zhu, Diesel fuel desulfurization with hydrogen peroxide promoted by formic acid and catalyzed by activated carbon, Carbon 43 (2005) 2285–2294.
[10] M.H. Ali, A. Al-Maliki, B. El-Ali, G. Martinie, M.N. Siddiqui, Deep desulfurization of gasoline and diesel fuels using non-hydrogen consuming techniques, Fuel 85 (2006) 1354–1363.
[11] H. Lu, J. Gao, Z. Jiang, F. Jing, Y. Yang, G. Wang, C. Li, Ultra-deep desulfurization of diesel by selective oxidation with $[C_{18}H_{37}N(CH_3)_3]_4[H_2NaPW_{10}O_{36}]$ catalyst assembled in emulsion droplets, J. Catal. 239 (2006) 369–375.
[12] B.H. Kim, H.Y. Kim, T.S. Kim, D.H. Park, Selectivity of desulfurization activity of *Desulfovibrio desulfuricans* M6 on different petroleum products, Fuel Process. Technol. 43 (1995) 87–94.
[13] D.J. Monticello, Biodesulfurization and the upgrading of petroleum distillates, Curr. Opin. Biotechnol. 11 (2000) 540–546.
[14] K.A. Gray, G.T. Mrachko, C.H. Squires, Biodesulfurization of fossil fuels, Curr. Opin. Microbiol. 6 (2003) 229–235.
[15] S. Guobin, Z. Huaiying, X. Jianmin, C. Guo, L. Wangliang, L. Huizhou, Biodesulfurization of hydrodesulfurized diesel oil with *Pseudomonas delafieldii* R-8 from high density culture, Biochem. Eng. J. 27 (2006) 305–309.
[16] G. Yu, S. Shanxiang Lu, H. Chen, Z. Zhu, Diesel fuel desulfurization with hydrogen peroxide promoted by formic acid and catalyzed by activated carbon, Carbon 43 (2005) 2285–2294.
[17] J. Weitkamp, M. Schwark, S. Ernst, Removal of thiophene impurities from benzene by selective adsorption in zeolite ZSM-5, J. Chem. Soc. Chem. Commun. (1991) 1133–1134.
[18] S.H.D. Lee, R. Kumar, M. Krumpelt, Sulfur removal from diesel fuel contaminated methanol, Sep. Purif. Technol. 26 (2002) 247–258.
[19] X. Ma, L. Sun, C. Song, A new approach to deep desulfurization of gasoline, diesel and jet fuel by selective adsorption for ultra-clean fuels and for fuel cell applications, Catal. Today 77 (2002) 107–116.
[20] A.J. Hernandez, R.T. Yang, New sorbents for desulfurization by selective adsorption via pi-complexation: sulfur removal from diesel fuels, AIChE J. 50 (2004) 791–801.
[21] Y. Sano, K. Sugaraha, K. Choi, Y. Korai, I. Mochida, Two-step adsorption process for deep desulfurization of diesel oil, Fuel 84 (2005) 903–910.
[22] W. Li, Q. Liu, J. Xing, H. Gao, X. Xiong, Y. Li, X. Li, H. Liu, High-efficiency desulfurization by adsorption with mesoporous aluminosilicates, AIChE J. 53 (2007) 3263–3268.
[23] A.K. Bajpai, M. Rajpoot, D.D. Mishra, Studies on the adsorption of sulfapyridine at the solution–alumina interface, J. Colloid Interface Sci. 187 (1997) 96–104.
[24] W. Wang, J.C.T. Kwak, Adsorption at the alumina–water interface from mixed surfactant solutions, Colloid Surf. A 156 (1999) 95–110.
[25] C.P. Huang, Adsorption of phosphate at the hydrous γ-Al_2O_3-electrolyte interface, J. Colloid Interface Sci. 53 (1975) 178–186.
[26] E. Baumgarten, U. Kirchhausen-Dusing, Sorption of metal ions on alumina, J. Colloid Interface Sci. 194 (1997) 1–9.
[27] T.P. Tranior, G.E. Brown Jr., G.A. Parks, Adsorption and precipitation of aqueous Zn(II) on alumina powders, J. Colloid Interface Sci. 231 (2000) 359–372.
[28] O. Etemadi, T.F. Yen, Surface characterization of adsorbents in ultrasound-assisted oxidative desulfurization process of fossil fuels, J. Colloid Interface Sci. 313 (2007) 18–25.
[29] J.H. Kim, X. Ma, A. Zhou, C. Song, Ultra-deep desulfurization and denitrogenation of diesel fuel by selective adsorption over three different adsorbents: a study on adsorptive selectivity and mechanism, Catal. Today 111 (2006) 74–83.
[30] IS 1350 (part I), Bureau of Indian Standards, Manak Bhawan, New Delhi, India (1984).
[31] E.P. Barret, L.G. Joyer, P.P. Halenda, The determination of pore volume and area distributions in porous substances: 1. Computations from nitrogen isotherms, J. Am. Chem. Soc. 73 (1951) 373–378.
[32] V.C. Srivastava, M.M. Swamy, I.D. Mall, B. Prasad, I.M. Mishra, Adsorptive removal of phenol by bagasse fly ash and activated carbon: equilibrium, kinetics and thermodynamics, Colloid Surf. A: Physicochem. Eng. Aspects 272 (2006) 89–104.
[33] G. Blanchard, M. Maunaye, G. Martin, Water Res. 18 (1984) 1501.
[34] Y.S. Ho, G. McKay, Pseudo-second order model for sorption processes, Process Biochem. 34 (1999) 451–465.
[35] W.J. Weber Jr., J.C. Morris, Kinetics of adsorption on carbon from solution, J. Sanitary Eng. Div. ASCE 89 (1963) 31–59.

[36] G.E. Boyd, A.W. Adamson, L.S. Meyers, The exchange adsorption of ions from aqueous solution by organic zeolites. II Kinetics, J. Am. Chem. Soc. 69 (1947) 2836–2848.
[37] A.H.P. Skelland, Diffusional Mass Transfer, Wiley, NY, 1974.
[38] V.C. Srivastava, I.D. Mall, I.M. Mishra, Modelling individual and competitive adsorption of cadmium(II) and zinc(II) metal ions from aqueous solution onto bagasse fly ash, Sep. Sci. Technol. 41 (2006) 2685–2710.
[39] H.M.F. Freundlich, Over the adsorption in solution, J. Phys. Chem. 57 (1906) 385–471.
[40] I. Langmuir, The adsorption of gases on plane surfaces of glass, mica and platinum, J. Am. Chem. Soc. 40 (1918) 1361–1403.
[41] O. Redlich, D.L. Peterson, A useful adsorption isotherm, J. Phys. Chem. 63 (1959) 1024–1026.
[42] M.I. Temkin, V. Pyzhev, Kinetics of ammonia synthesis on promoted iron catalysts, Acta Physiochim. URSS 12 (1940) 327–356.
[43] D.W. Marquardt, An algorithm for least-squares estimation of nonlinear parameters, J. Soc. (Ind) Appl. Math. 11 (1963) 431–441.
[44] R. Aravindhan, J.R. Rao, B.U. Nair, Removal of basic yellow dye from aqueous solution by sorption on green alga *Caulerpa scalpelliformis*, J. Hazard. Mater. 142 (2007) 68–76.
[45] G. McKay, S.J. Allen, I.F. McConvey, M.S. Otterburn, Transport process in the sorption of colored ions by peat particles, J. Colloid Interface Sci. 80 (2) (1981) 323–339.
[46] D. Reichenberg, Properties of ion-exchange resin in relation to their structure. III. Kinetics of exchange, J. Am. Chem. Soc. 75 (1953) 587–589.
[47] J. Crank, The Mathematics of Diffusion, 1st ed., Oxford Clarendon Press, London, 1965.
[48] A.K. Chaturvedi, K.C. Pathak, V.N. Singh, Fluoride removal from water by adsorption on china clay, Appl. Clay Sci. 3 (1988) 337–346.
[49] H.L. Wang, W.F. Jiang, Adsorption of dinitro butyl phenol (DNBP) from aqueous solutions by fly ash, Ind. Eng. Chem. Res. 46 (2007) 5405–5411.
[50] L.D. Landau, E.M. Lifshitz, Statistical Physics, Pergamon Press, Oxford, UK, 1980.